

# AN INVESTIGATION INTO THE EFFICACY OF GRAPHENE OXIDES AS AN ADSORBENT FOR THE REMOVAL OF LEAD FROM AQUEOUS SOLUTION

Nwe Nwe Win<sup>1</sup>, Thazin Nyo<sup>2</sup>, Ohn Ohn Soe<sup>3</sup>

## Abstract

Heavy metals are a concern in the environment as they accumulate and are non-biodegradable and thus bio-toxic. Many technologies have been employed for the removal of heavy metals in the environment. However, adsorption process is arguably the most promising and effective fundamental approach for the removal of heavy metals in wastewater treatment processes. An effective and facial method for removal of Pb<sup>2+</sup> ion from aqueous solution is based on the prepared graphene oxides. The oxygenous functional groups on the surface of graphene oxides were primarily responsible for the sorption of metal ions. The graphene oxides were prepared from different graphite sources using modified Hummer's method. The prepared graphene oxides (LGO, CGO, FGO) were used as adsorbent for removal of heavy metal ion (Pb<sup>2+</sup> ion). The different graphite varieties (LGP, CGP, FGP) and the prepared graphene oxides (LGO, CGO, FGO) were characterized by XRD, UV-vis, FT IR and SEM. To obtain the optimum parameters for the removal of Pb<sup>2+</sup> ion from model aqueous solution, adsorbent dosage, Pb<sup>2+</sup> ion concentration and contact time were examined by complexometric titration method. The maximum removal capacity of Pb<sup>2+</sup> ion using LGO, CGO and FGO were found to be 94.60 %, 95.66 % and 87.32 % at their optimal conditions. The removal capacity of Pb<sup>2+</sup> ion on CGO and LGO was not quite different but FGO was lower than the other two. The obtained results demonstrated that the prepared graphene oxides can be used as an effective adsorbent for Pb<sup>2+</sup> ion removal from water.

**Keywords:** Graphite, graphene oxide, modified Hummer's method, heavy metal and adsorption capacity

## Introduction

Water pollution due to the indiscriminate disposal of metal ions and organic contaminants has been a rising worldwide environmental concern (Madadrang *et al.*, 2012). Heavy metals are among the most common pollutants found in wastewater and can be accumulated in the environmental and living tissues, causing various diseases and disordering of living organisms even at a trace level (Chen *et al.*, 2016). Pb (II) is one of the most toxic heavy metals, which is generated by mining, electroplating, dyeing, battery, textile, explosive, and other industries. Lead poisoning can bring serious risks to kidney, liver, blood, nerve, and reproductive systems, causing symptoms as anemia, chronic headache, dysentery, amentia, etc (Guo *et al.*, 2018). For environmental protection, it is necessary to remove these metal contaminants from the wastewater before releasing into the environment. Entire removal of heavy metals and organic contaminants in natural water resources can not only protect the environment itself, but also stop the toxic contaminant transfer in food chains (Madadrang *et al.*, 2012). Many technologies and methods for heavy metals ions removal from waste waters have been developed, such as ion-exchange, evaporation and concentration, chemical precipitation, reverse osmosis, adsorption, and electro dialysis (Mi *et al.*, 2012). Adsorption is the most extensively used method due to its simplicity, flexibility, insensitivity to toxic substances, high efficiency in large scale applications and low cost (Shaaban *et al.*, 2019). Graphene oxide (GO) offers interesting properties such as hydrophilicity due to the presence of carboxylic functional groups and epoxy groups essential for high sorption capacity. This material has gained importance in portable and wastewater treatment due to its

---

<sup>1</sup> 3 PhD-Chem-8, Department of Chemistry, University of Yangon

<sup>2</sup> Dr, Lecturer, Department of Chemistry, Dagon University

<sup>3</sup> Dr, Associate Professor, Department of Chemistry, Loikaw University

extraordinary properties such as its high adsorption capacity and catalysis efficiency (Khumalo *et al.*, 2017).

In this paper, the optimal conditions of  $\text{Pb}^{2+}$  ion adsorption by GO were determined such as dosage, concentration and contact time.

## Materials and Methods

### Materials

In this research, local graphite (LGP) was collected from Lin-yaung-chi mine, Mogok Township. Commercial graphite (CGP) was purchased from local chemical shop and flake graphite (FGP) was also purchased from Alfa Aesar Company, Japan. They were used without further purification. All chemicals used were of analytical reagent grade.

### Preparation of Stock and Standard Solutions of Lead (II) nitrate Solution

1.615 g of 99 %  $\text{Pb}(\text{NO}_3)_2$  was dissolved in distilled water in 1 L volumetric flask up to the mark to obtain 1000 ppm of lead stock solution. By serial dilution, the  $\text{Pb}^{2+}$  solution 200 ppm was prepared.

### Preparation of Graphene Oxides

Each graphene oxide was prepared according to the modified Hummer's method (Song *et al.*, 2014). 5 g of graphite and 2.5 g of  $\text{NaNO}_3$  were mixed with 108 mL  $\text{H}_2\text{SO}_4$  and 12 mL  $\text{H}_3\text{PO}_4$  and stirred in an ice bath for 10 min. Next, 15 g of  $\text{KMnO}_4$  was slowly added and the temperature of the mixture remained below 5 °C. The suspension was then reacted for 2 h in an ice bath and stirred for 60 min before again being stirred in a 40 °C water bath for 60 min. The temperature of the mixture was adjusted to a constant 98 °C for 60 min while water was added continuously. Deionized water was further added so that the volume of the suspension was 400 mL. After 5 min, 15 mL of  $\text{H}_2\text{O}_2$  was added to stop oxidation reaction and to reduce excess  $\text{KMnO}_4$  and the colour of mixture changed to brilliant yellow. The reaction product was washed with deionized water to remove the acid and with 5 % HCl solution repeatedly to remove metal ions. The GO gel-like layer starts appearing when the pH of the supernatant is neutralized, after several centrifugation rounds. Finally, the product was dried at 60 °C.

### Characterization of Different Graphite and the Prepared Graphene Oxides by XRD, UV-Vis, FT IR and SEM

The different graphite varieties (LGP, CGP and FGP) and prepared graphene oxides (LGO, CGO and FGO) were characterized by XRD, UV-Vis, FT IR and SEM.

### Batch Adsorption Experiments

The adsorption experiments were conducted using batch technique. In all, 1.615 g of 99 %  $\text{Pb}(\text{NO}_3)_2$  was dissolved in 1000 mL distilled water to obtain a solution with  $\text{Pb}^{2+}$  concentration of 1000  $\text{mgL}^{-1}$ . Experimental solutions of the desired concentration were obtained by further dilution. Measurements of the lead ion solutions with known concentrations of 50 to 350 ppm were conducted to optimize dosage and contact time. A certain dosage of LGO, CGO and FGO was added into the  $\text{Pb}^{2+}$  solution, then the flask was shaking under a room temperature and a fixed rotation speed of 150 rpm in a shaker. After completing a certain contact time, the prepared graphene oxides were separated from  $\text{Pb}^{2+}$  solution by filtration. The resultant filtrates were

analyzed by complexometric titration. All of the samples were tested by triplicated and all the experiments were also performed at room temperature. The removal efficiency was calculated by the following equation:

$$R \% = C_0 - C_e / C_0 \times 100$$

Where,  $C_0$  and  $C_e$  are the initial and equilibrium metal ion concentration (ppm) in the aliquots, respectively (Shaaban *et al.*, 2019).

### Titration Procedure

200 ppm of  $Pb^{2+}$  ion solution, 10 cm<sup>3</sup> of 9 % hexamethylenetetramine and 4 cm<sup>3</sup> of 0.01 % (w/v) xylenol orange indicator solution were added. The pH of this mixed solution was adjusted with a 0.01 M NaOH or 0.01 M HNO<sub>3</sub> (pH 5.6). The mixed solution was titrated with 0.01 M EDTA solution.

## Results and Discussion

### XRD Analysis

The crystalline structures of different graphite varieties and prepared graphene oxides were characterized by XRD. The X-ray Diffraction patterns (XRD) of LGP, CGP, FGP and prepared graphene oxides (LGO, CGO, FGO) were shown in Figure 1 and Table 1. The sharp peaks of graphite LGP, CGP, FGP at  $2\theta=27.44^\circ$  ( $d=0.3248$  nm),  $2\theta=26.609^\circ$  ( $d=0.3347$  nm),  $2\theta=26.485^\circ$  ( $d=0.3362$  nm) corresponding to the plane (002), that shifts to  $2\theta=10.104^\circ$  ( $d=0.8747$  nm),  $2\theta=10.557^\circ$  ( $d=0.8373$  nm),  $2\theta=10.394^\circ$  ( $d=0.8504$  nm) on chemical oxidation, confirming the formation of prepared graphene oxides (LGO, CGO, FGO). The crystallite sizes 5.13 nm, 4.05 nm and 5.33 nm can be assigned to the LGO, CGO and FGO, respectively. The increase in interlayer spacing from different graphite varieties to prepared graphene oxides is due to the introduction of the various functional groups that have been introduced by the oxidation of graphite.

### UV-Visible Analysis

The UV-vis spectroscopic measurement was carried out in the range of (200 – 400) nm to monitor the graphite samples and the degree of oxidation for the graphene oxide samples. The UV-visible spectra were shown in Figures 2 (a, b, c). The maximum  $\pi-\pi^*$  transition of C = C, C - C peaks of LGP, CGP and FGP were found ( $\lambda=258.0$  nm,  $\lambda=267.3$  nm and  $\lambda=296.1$  nm). From UV-vis spectroscopic studies, Figure 2 (d, e, f), it can be inferred that the optical absorption of LGO, CGO, FGO were dominated by the  $\pi-\pi^*$  plasmon peak near (201.6 nm, 204.2 nm, 200.8 nm). The shoulder peak at (311.2 nm, 307.6 nm, 307.8 nm) revealed for n -  $\pi^*$  transitions of C = O bond from oxidized carbon of LGO, CGO and FGO. The  $\pi-\pi^*$  plasmon peak depends on two kinds of conjugative effect: one is related to nanometer-scale  $sp^2$  clusters, and the other arises from linking chromophore units such as C =C, C =O and C–O bonds. This result clearly indicated in Table 2.

### FT IR Analysis

The FT IR analysis can be one of the direct evidences for the different graphite varieties and prepared graphene oxides as it provides information about the functional groups that present in the samples. The spectra of LGP, CGP and FGP showed typical peaks of broad band at 3624 cm<sup>-1</sup>, 3703 cm<sup>-1</sup>, 3726 cm<sup>-1</sup> related to the O-H (free and carboxylic), while the peaks at 1639 cm<sup>-1</sup>, (1479, 1037, 1033, 941, 912) cm<sup>-1</sup> and (794, 690, 540, 528, 468, 466, 414) cm<sup>-1</sup> arise from the stretching vibration of C=C, C-H in plane bending and C-H out of plane deformation of benzene. The spectra of the prepared graphene oxides illustrated absorption peaks at (3347, 3692,

3443)  $\text{cm}^{-1}$  assigned to hydroxyl groups, (3242, 3053)  $\text{cm}^{-1}$  attributed to C-H stretching vibration, (1726, 1581, 1609)  $\text{cm}^{-1}$  corresponded to C=O stretching vibrations in the carbonyl. The peak at 1548  $\text{cm}^{-1}$  is due to C=C in aromatic ring while 1377  $\text{cm}^{-1}$  corresponded to C-O stretching of carboxylic acid. 1242  $\text{cm}^{-1}$  and 1315  $\text{cm}^{-1}$  are for C-O-C stretching vibration of epoxide, 1128  $\text{cm}^{-1}$  are C-O stretching of alcohol group. The peaks at (1030, 1003, 925, 912)  $\text{cm}^{-1}$  are C-H in plane bending and (680, 584)  $\text{cm}^{-1}$  are C-H out of plane deformation of benzene, respectively. These results were shown in Figure 3 and Table 3.

### SEM Analysis

Surface morphologies of the different graphite varieties and the prepared graphene oxides were determined by using SEM and the micrographs were shown in Figure 4. Figure 4 (a, b, c) are platelet like crystalline form of carbon. Figure 4 (d) showed the SEM image of LGO which resembled randomly aggregated, thin crumpled sheets closely associated with each other and forming a disordered solid. Figure 4 (e) shows that CGO image revealed the crumpled and ripple structure which was the result of deformation upon the exfoliation and restacking processes. Figure 4 (f) shows SEM image of FGO. The morphology of FGO appears as a tightly packed layer with a corrugate surface that sometimes is wrinkled.

### Batch Adsorption Study

The batch experiments were done by studying different parameters.

#### Effect of dosage of adsorbent

The effect of dosages on the adsorption properties was investigated in the range 0.02 g to 0.14 g. Table 4 shows the corresponding data in terms of percent removal with respect to adsorbent doses. The optimal dosages were occurred at 0.08 g for (LGO, FGO), and 0.06 g for (CGO). The maximum removal percent were occurred at 92.57 % for LGO, 93.60 % for CGO and 84.30 % for FGO, respectively. Figure 5 shows the number of active sites available for adsorption increase as the adsorbent dosage increase, providing  $\text{Pb}^{2+}$  ion more probabilities to be adsorbed, consequently leading to increase of the adsorption percent. The higher the adsorbent dose is attributed to the particle interactions such as aggregation. This aggregation would lead to a decrease in the total surface area of the adsorbent. The increase of the adsorbent dosage, the adsorption percent increase, while the adsorption quantity decreased, respectively.

#### Effect of initial concentration of $\text{Pb}^{2+}$ ion

The removal of  $\text{Pb}^{2+}$  ion was performed using various initial concentrations from 50 ppm to 350 ppm at 30 min. Table 5 and Figure 6 show the removal of  $\text{Pb}^{2+}$  ion from aqueous solution. The maximum removal efficiencies were occurred at 250 ppm for all samples. The results indicate that the equilibrium sorption capacities of the sorbent increase with increasing the initial  $\text{Pb}^{2+}$  ion concentration due to the strong driving force of the concentration gradient at solid-liquid interface which causes an increase of the amount of metal ions adsorbed on the adsorbent. At low concentration of initial metal ions sufficient adsorption sites are available for the heavy metal ions and as the initial concentration of metal ions increases, more and more surface sites are covered and at high concentration of the metal ions, the capacity of the adsorbent get exhausted due to the non-availability of the surface sites.

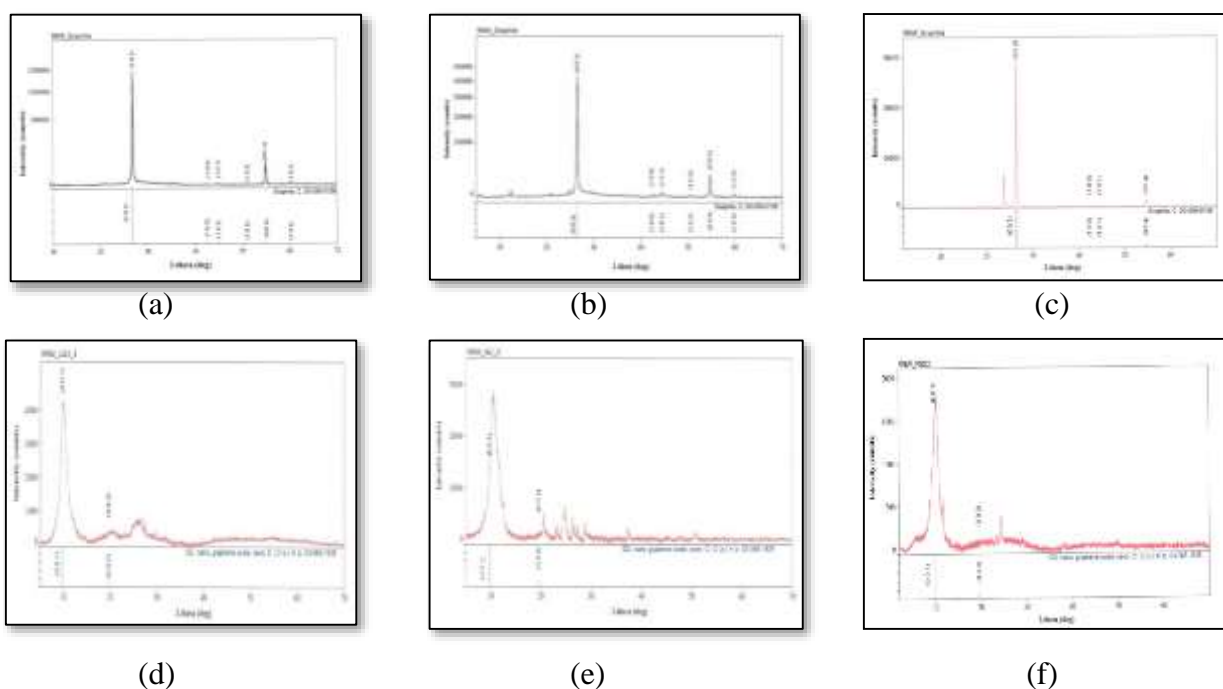
#### Effect of contact time

The influence of adsorption time intervals on the uptake capacities of the prepared graphene oxides was investigated. The contact time was varied between 15 min to 105 min. The time required to achieve the adsorption equilibrium were 60 min for LGO, 30 min for CGO and 75 min

for FGO, respectively. This can be attributed to the large surface area the sufficient exposure of active sites and the high surface reactivity of the graphene oxides. This data was shown in Table 6 and Figure 7.

**Effect of optimal parameters on Pb<sup>2+</sup> ion removal**

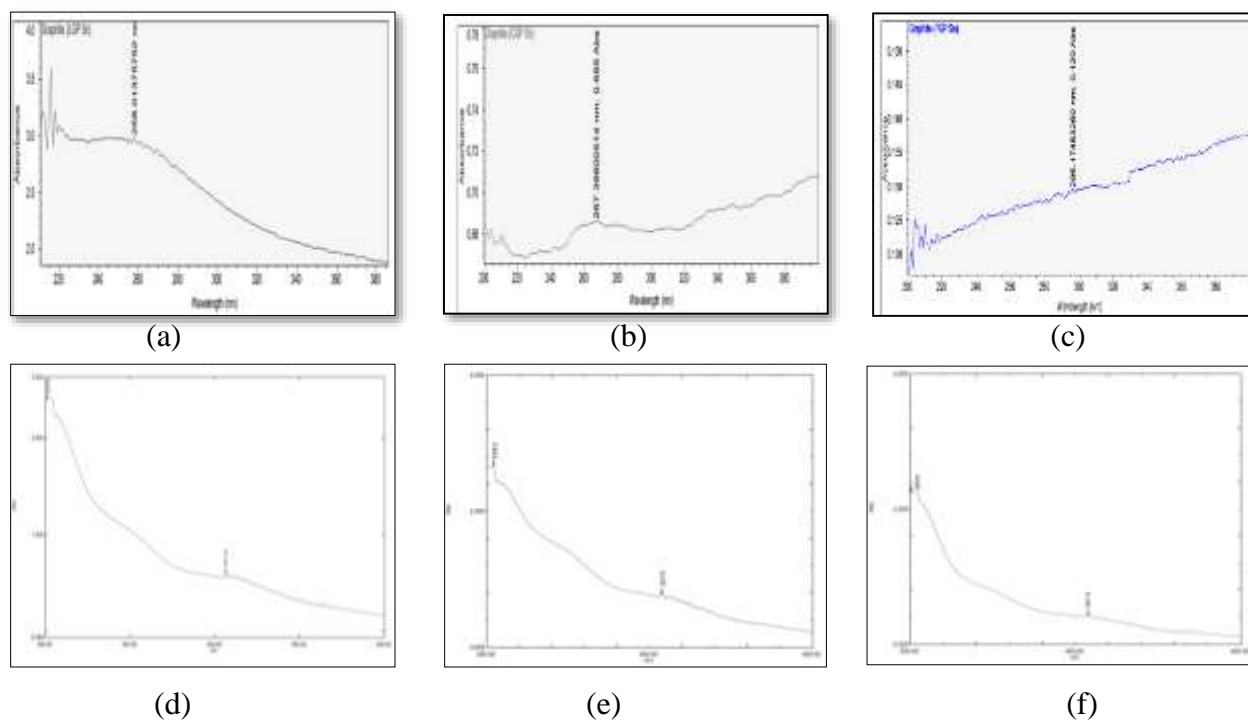
Ability of graphene oxides as adsorbent was influenced by optimal parameters. Maximum adsorption experiments were carried out at optimal condition, including adsorbent dosage, concentration of metal ion and contact time. Table 7 and Figure 8 show the maximum removal percent of Pb<sup>2+</sup> ion under comparable conditions. The maximum removal percent efficiency of Pb<sup>2+</sup> ion 94.60 %, 95.66 % and 87.32 % were found by using 0.08 g of LGO, 0.06 g of CGO and 0.08 g of FGO in 250 ppm of Pb<sup>2+</sup> ion. The optimal contact times of LGO, CGO and FGO were 60 min, 30 min and 75 min. So, CGO had a high potential for heavy metal removing compared with LGO and FGO adsorbents. Results show that the adsorption equilibrium, the removal efficiencies were nearly 96 %. Among graphene oxide samples, CGO is an excellent adsorbent for removal of heavy metal ions.



**Figure 1** XRD diffractograms of (a) LGP (b) CGP (c) FGP (d) LGO (e) CGO and (f) FGO

**Table 1** Phase Identification of LGP, CGP, FGP, LGO, CGO and FGO

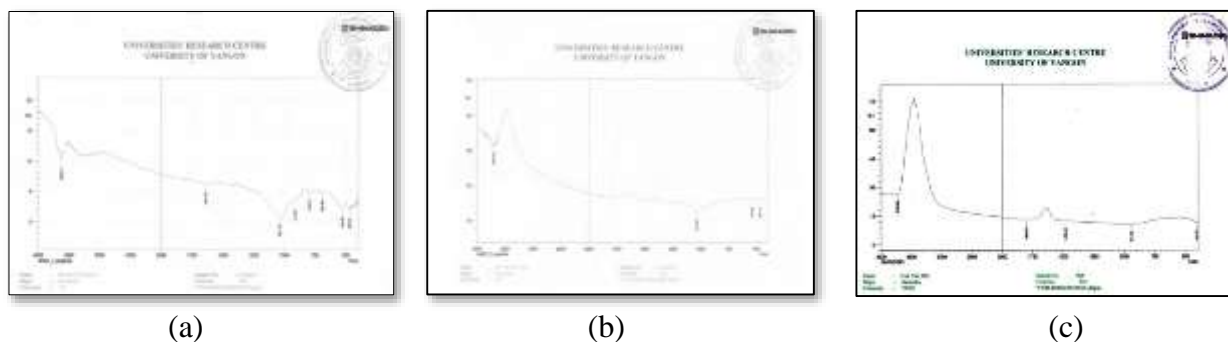
Samples	Miller Indies (h k l)	Bragg angle (2θ) Degree	Interplannar spacing d (nm)	Phase Identification	Crystallite size (nm)
LGP	0 0 2	27.44	0.3248	Graphite	56.0
CGP	0 0 2	26.609	0.3347	Graphite	40.3
FGP	0 0 2	26.485	0.3362	Graphite	33.43
LGO	0 0 1	10.104	0.8747	Graphene oxide	5.13
CGO	0 0 1	10.557	0.8373	Graphene oxide	4.05
FGO	0 0 1	10.394	0.8504	Graphene oxide	5.33



**Figure 2** UV-Vis spectra of (a) LGP (b) CGP (c) FGP, (d) LGO, (e) CGO and (f) FGO

**Table 2** UV-Vis Analysis of LGP, CGP, FGP, LGO, CGO and FGO

Samples	Wavelength (nm)	Band Assignment
LGP	258.0	$\pi$ - $\pi^*$ transition of C = C, C - C
CGP	267.3	$\pi$ - $\pi^*$ transition of C = C, C - C
FGP	296.1	$\pi$ - $\pi^*$ transition of C = C, C - C
LGO	{ 201.6 311.2	$\pi$ - $\pi^*$ transition of C = C, C - C
		n- $\pi^*$ transition of C = O
CGO	{ 204.2 307.6	$\pi$ - $\pi^*$ transition of C = C, C - C
		n- $\pi^*$ transition of C = O
FGO	{ 200.8 307.8	$\pi$ - $\pi^*$ transition of C = C, C - C
		n- $\pi^*$ transition of C = O



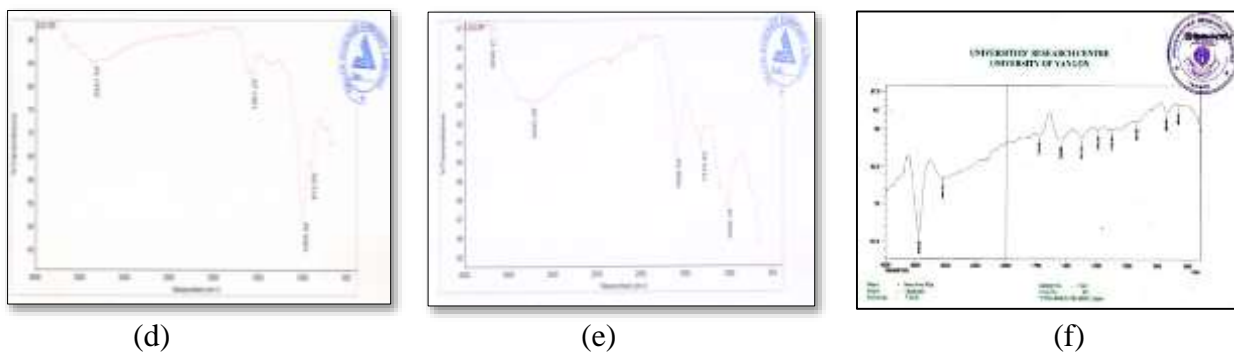
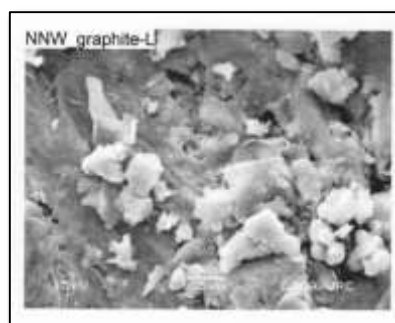


Figure 3 FT IR spectra of (a) LGP (b) CGP (c) FGP, (d) LGO (e) CGO and (f) FGO

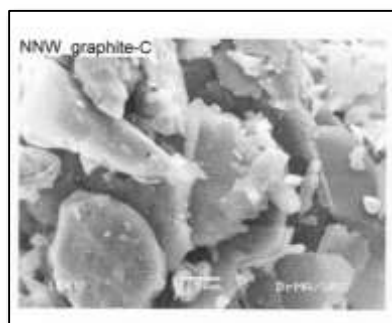
Table 3 Assignment of FT IR Spectra Data of LGP, CGP, FGP, LGO, CGO and FGO

No.	Observed value (cm <sup>-1</sup> )						Literature values* (cm <sup>-1</sup> )	Band Assignment
	LGP	CGP	FGP	LGO	CGO	FGO		
1	3624	3703	3726	3347	3692	3443	3200-3600	OH stretching vibration
2					3243			
3	-	-	-	-	-	3053	3000-3100	C-H stretching vibration
4	1639	-	-	-	-	-	1600-1750	C=C stretching vibration
5	-	-	-	1581	1609	1726	1540-1870	C=O stretching in carbonyl
6	-	-	-	-	-	1548	1500-1600	C=C stretching vibration
7	-	-	-	-	-	1377	1385	C-O stretching of carboxylic acid
8	-	-	-	-	1315	1242	1230-1320	C-O-C stretching vibration of epoxide
9	-	-	-	-	-	1128	1087-1124	C-O stretching of alcohol group
10	1037	1033	1479	1003	1030	-925	990-1790	C-H in plane bending
11	912							
12	794	540	414	-	-	680	450-750	C-H out of plane deformation (benzene)
13	690							
14	528							
15	468							
	466							

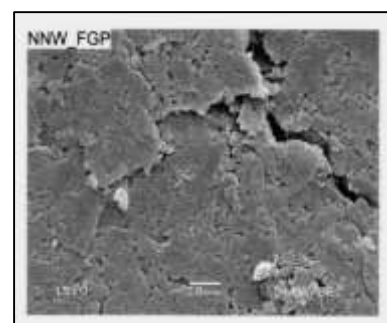
\*Sun et al., 2011



(a)



(b)



(c)

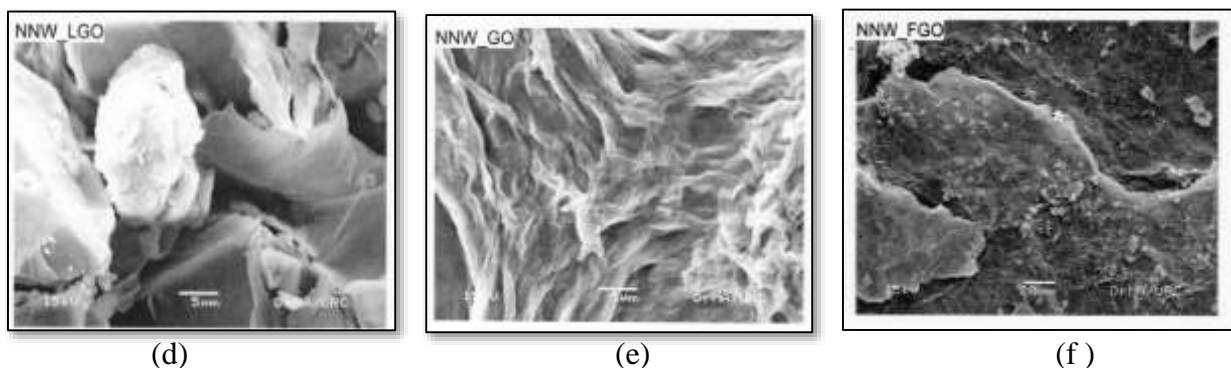
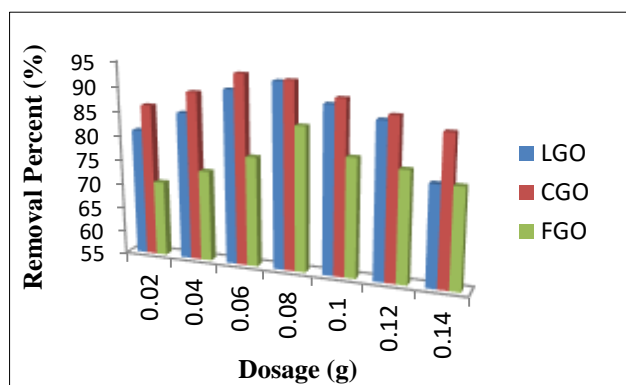


Figure 4 SEM micrographs of (a) LGP (b) CGP (c) FGP (d) LGO (e) CGO and (f) FGO

Table 4 Removal Percent of  $Pb^{2+}$  Ion by Using Different Graphene Oxides (LGO, CGO, FGO) as a Function of Dosages

No.	Weight of Dosage (g)	Removal Percent (%)		
		LGO	CGO	FGO
1	0.02	80.85 ± 2.82	86.12 ± 4.24	70.36 ± 2.82
2	0.04	85.09 ± 1.41	89.40 ± 5.65	73.57 ± 1.41
3	0.06	90.35 ± 1.41	93.60 ± 1.41	77.35 ± 1.41
4	0.08	92.57 ± 2.82	92.85 ± 4.24	84.30 ± 1.41
5	0.10	88.82 ± 1.41	90.09 ± 2.82	79.03 ± 2.82
6	0.12	86.54 ± 2.82	87.57 ± 1.41	77.57 ± 1.41
7	0.14	75.37 ± 0.70	85.20 ± 0.70	75.37 ± 7.37



Experimental condition

Contact time = 30 min  
 Temperature = RT  
 $Pb^{2+}$  ion Concentration = 200 ppm  
 Stirring rate = 150 rpm  
 Volume of solution = 50 mL

Figure 5 Removal percent of  $Pb^{2+}$  ion solution by different graphene oxides as a function of dosages

Table 5 Removal Percent of  $Pb^{2+}$  Ion by Using Different Graphene Oxides (LGO, CGO, FGO) as a Function of Concentrations

No.	Concentration of $Pb^{2+}$ ion solution (ppm)	Removal Percent (%)		
		LGO	CGO	FGO
1	50	79.82 ± 6.25	83.08 ± 4.41	71.87 ± 4.42
2	100	81.79 ± 9.51	85.02 ± 6.34	73.12 ± 3.17
3	150	85.92 ± 3.45	91.54 ± 1.67	79.46 ± 1.72
4	200	92.81 ± 4.24	93.12 ± 1.42	84.76 ± 2.82
5	250	93.52 ± 3.13	95.08 ± 5.19	85.03 ± 3.11
6	300	86.58 ± 3.06	89.02 ± 6.16	84.58 ± 3.35
7	350	83.03 ± 4.15	86.54 ± 1.22	81.03 ± 2.34





**Figure 6** Removal percent of Pb<sup>2+</sup> ion solution by different graphene oxides as a function of concentrations

**Table 6** Removal Percent of Pb<sup>2+</sup> Ion Solution by Using Different Graphene Oxides (LGO, CGO, FGO) as a Function of Contact Times

No.	Contact Time (min)	Removal Percent (%)		
		LGO	CGO	FGO
1	15	84.05 ± 1.50	88.18 ± 12.72	79.19 ± 8.17
2	30	92.85 ± 4.48	95.21 ± 2.82	84.92 ± 4.24
3	45	93.84 ± 2.82	93.16 ± 1.41	85.49 ± 5.65
4	60	94.12 ± 3.10	92.61 ± 9.89	86.51 ± 1.41
5	75	82.32 ± 2.82	89.68 ± 4.24	87.15 ± 1.41
6	90	80.36 ± 7.07	88.35 ± 1.41	84.21 ± 5.65
7	105	79.12 ± 2.82	87.46 ± 2.82	82.70 ± 7.07

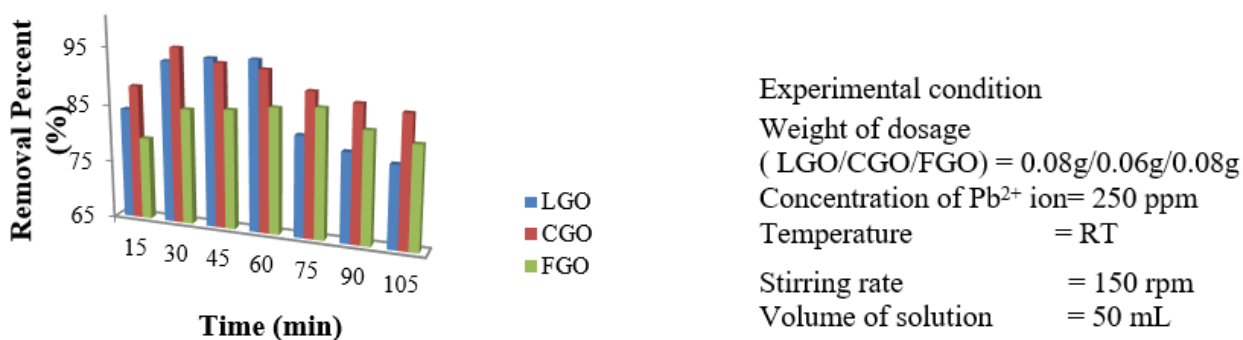


**Figure 7** Removal percent of Pb<sup>2+</sup> ion solution by graphene oxides (LGO, CGO, FGO) as a function of contact times

**Table 7** Removal of Pb<sup>2+</sup> Ion by Prepared Graphene Oxides (LGO, CGO, FGO) at Optimal Conditions

Sample	Dosage (g)	Pb <sup>2+</sup> Ion Concentration (ppm)	Time (min)	Removal Percent (%)
LGO	0.08	250	60	94.60 ± 0.16
CGO	0.06	250	30	95.66 ± 0.41
FGO	0.08	250	75	87.32 ± 0.15

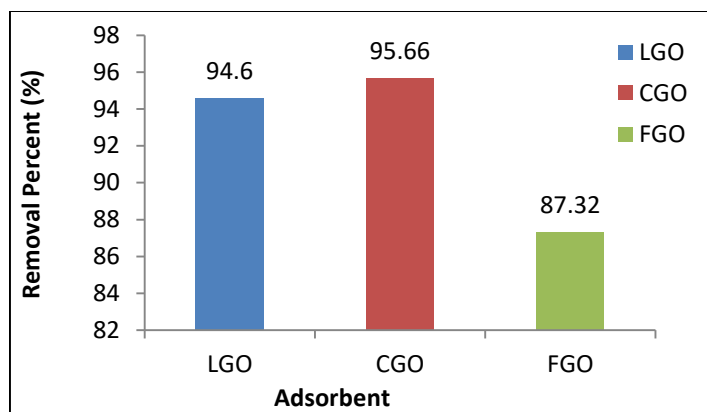


**Figure 8** The optimal parameters of prepared graphene oxides (LGO, CGO, FGO) for removal of  $Pb^{2+}$  ion

### Conclusion

The result of graphene oxide materials in adsorption indicates that it has a great future in the decontamination of water. The efficiency of these materials on the removal of heavy metals ( $Pb^{2+}$ ) from contaminated water will be depending on factors such as dosage, initial concentration of metal ion, and contact time. The presence of oxygen-containing groups and characteristic peaks in FT-IR and XRD analysis indicated the successful preparation of GO sheets. Among the prepared graphene oxides, CGO showed successfully removed nearly 95.66 % of heavy metal ion ( $Pb^{2+}$  ion) from aqueous solution under optimum experimental conditions of 250 ppm of  $Pb^{2+}$ , adsorbent dosage of 0.06 g and contact time of 30 min. CGO is highly recommended to be used in water treatment for its high adsorption capacity followed by LGO and FGO. So, CGO is an excellent adsorbent for removal of heavy metal ions. Thus, CGO can be considered the most effective adsorbent on the removal of  $Pb^{2+}$  ion from aqueous solution.

### Acknowledgements

The authors would like to thank the Myanmar Academy of Art and Science for allowing to present this paper and Professor and Head Dr Ni Ni Than, Department of Chemistry, University of Yangon, for her kind encouragement.

### References

- Chen, X., Zhou, S., Zhang, L., You, T. and Xu, F. (2016). "Adsorption of Heavy Metals by Graphene Oxide/Cellulose Hydrogel Prepared from NaOH/Urea Aqueous Solution". *Materials*, vol. 9(582), pp.1-15.
- Guo, T., Bulin, C., Li, B., Zhao, Z., Yu, H., Sun, He., Ge, X., Xing, R. and Zhang, B. (2018). "Efficient Removal of Aqueous Pb (II) Using Partially Reduced Graphene Oxide- $Fe_3O_4$ ". *Adsorption Science & Technology*, vol. 36(3-4), pp. 1031-1048.
- Khumalo, N. P., Mhlanga, S. D., Kuvarega, A. T., Vilakati, G. D., Mamba, B. B. and Dlamini, D. S. (2017). "Adsorptive Removal of Heavy Metals from Aqueous Solution by Graphene Oxide Modified Membranes". *International Journal of Scientific & Engineering Research*, vol. 8(4), pp. 1184-1194.
- Madadrang, C. J., Kim, H. Y., Gao, G., Wang, N., Zhu, J., Feng, H., Gorrington, M., Kasner, M. L. and Hou, S. (2012). "Adsorption Behavior of EDTA-Graphene Oxide for Pb (II) Removal". *ACS Applied Materials & Interfaces*, vol. 4, pp. 1186-1193.
- Mi, X., Huang, G., Xie, W., Wang, W., Liu, Y. and Gao, J. (2012). "Preparation of Graphene Oxide Aerogel and Its Adsorption for  $Cu^{2+}$  Ions". *Carbon*, vol. 50, pp. 4856-4864.
- Shaaban, A. F., Khalil, A. A., Elewa, B. S., Ismail, M. N. and Eldemerdash, U. M. (2019). "A New Modified Exfoliated Graphene Oxide for Removal of Copper (II), Lead (II) and Nickel (II) Ions from Aqueous Solutions". *Egyptian Journal of Chemistry*, vol. 62(10), pp. 1823-1849.
- Song, J., Wang, X. and Chang, C. T. (2014). "Preparation and Characterization of Graphene Oxide". *Journal of Materials*, vol. 2014, pp. 1-6.
- Sun, H., Yang, Y. and Huang, Q. (2011). "Preparation and Structural Variation of Graphite Oxide and Graphene Oxide". *Integrated Ferroelectrics an International Journal*, vol. 128, pp. 163-170.